Coronal mass ejections and space weather due to extreme events

N. Gopalswamy[1], S. Yashiro[1,2] and S. Akiyama[1,2]

[1]NASA Laboratory for Extraterrestrial Physics, NASA Goddard Space Flight Center, Code 695.0, Greenbelt, MD 20771, USA
[2] The Catholic University of America, Washington DC 20064, USA

Abstract. This paper summarizes the extreme solar activity and its space weather implications during the declining phase of the solar cycle 23: October-November 2003 (AR 486), November 2004 (AR 696), January 2005 (AR 720), and September 2005 (AR 808). We have compiled and compared the properties of eruptions and the underlying active regions. All these are super active regions, but the flare and CME productivity varied significantly. While the CMEs from all the regions kept the level of solar energetic particles (SEPs) at storm level for several days, their geoeffectiveness (the ability to produce geomagnetic storms) was significantly different, probably due to the location of the eruptions on the Sun.

Index Terms. Coronal mass ejection, magnetic field reconnection, solar wind plasma, solar-terrestrial relations.

1. Introduction

Geoeffective coronal mass ejections (CMEs) have the ability to significantly disturb geospace, when the CME plasma arrives at Earth (see Howard et al., 1982; Gosling, 1993). The geoeffectiveness is typically assessed using the "disturbance storm" index or Dst. When Dst < -50 nT the storm is considered to be significant (see Tsurutani and Gonzalez, 1988; Webb et al., 2000). CMEs also can result in significant levels of solar energetic particles (SEPs) at Earth (Reames, 1999). When the >10 MeV proton intensity exceeds 10 particle flux units (pfu = particles·cm^{-2}s^{-1}sr^{-1}) the particle events are significant and the associated CMEs are considered SEPeffective. There is another phenomenon, which depends on the combination of plasma arrival and SEP production: the energetic storm particle (ESP) events (see Cohen, 2006 for a review). During an ESP event, the CME-driven shock arrives at the observing spacecraft, accelerating energetic particles (whose intensity could increase by an order of magnitude compared to the intensity before the shock arrival). The shock impact on the magnetosphere also marks the first instance of a CME-related disturbance arriving at Earth and is known as sudden commencement. The geomagnetic storm can start any time after the shock arrival depending on the availability of the southward component of the magnetic field in the shock sheath and/or in the CME that follows. The geoeffective and SEPeffective CMEs constitute a small population compared to all the CMEs and are typically associated with large flares. The X-ray and EUV emission from the flares reach Earth's atmosphere in about 8 minutes causing extra ionization in the ionosphere. Thus the arrival of plasmas, particles and electromagnetic radiation decides the lead times available for space weather forecast. One has to consider various time scales, depending on the space weather application one is interested in. While the arrival of SEPs and flare emission is too quick to be predicted after an eruption occurs, the prediction of the arrival of shocks and CMEs should be possible. For flares and SEPs, the prediction must focus on whether an active region on the disk will produce an eruption. For CMEs and shocks, one can predict the shock and CME arrival soon after the eruption has occurred.

The source regions of the SEPeffective CMEs are generally located on the western hemisphere, although occasionally they do originate from the eastern hemisphere. The geoeffective CMEs, on the other hand, originate close to the disk center. Thus, the union of the two sets (most of the front- sided fast and wide CMEs) is important in deciding the conditions in Earth's space environment, but the intersection of the sets define the most important CMEs (producing both SEP events and geomagnetic storms).

In this paper, we report on a set of space weather events that occurred during the declining phase of solar cycle 23. These events were observed with a large array of ground and space-based observatories allowing in-depth analyses. Such analyses are important in assessing the severity of the events and set limits to the level of impact they can produce at Earth. The events considered in this paper correspond to four intervals: (1) October-November 2003 (Halloween storms), (2) November 2004, (3) January 2005, and September 2005. The 2003 Halloween events have been extensively studied and reported (see Gopalswamy et al., 2005a for a list of several dozen papers published recently). Here we use them to compare with the other sets of events.

2. Super active regions

There have been many active regions, which produced large numbers of intense flares and CMEs during solar cycle 23. When these happen close to the disk center and in the

western hemisphere, they impact geospace with geomagnetic storms and solar energetic particles. These events have significant implications for space weather. Fig. 1 shows the CME rate and the mean speed (averaged over Carrington rotations) of all the CMEs detected by the Solar and Heliospheric Observatory (SOHO) mission's Large Angle and Spectrometric Coronagraph (LASCO). The CME rate and mean speed show lots of fluctuations corresponding to solar sources often producing large number of CMEs. The mean speed has some distinct spikes with very high speeds. Several of these were active regions that produced large number of flares and fast CMEs. Some familiar active regions are marked in the figure. The regions discussed in this paper belong to the declining phase of cycle 23 (the last four spikes).

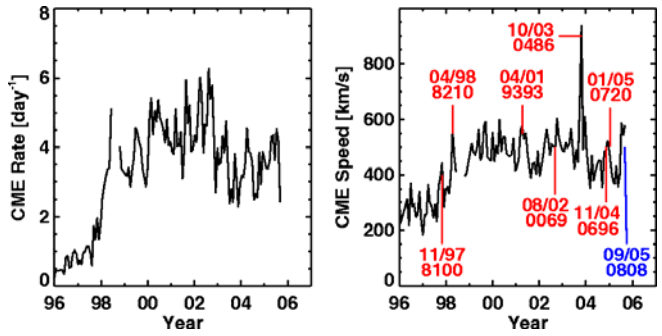

Fig. 1. The CME rate and mean speed (averaged over Carrington Rotation periods) as a function of time from 1996 to the end of September 2005. The large spikes in the mean speed plot are indicative of super events. Higher mean speed enhances the likelihood for geoeffectiveness.

The October-November 2003 period witnessed solar eruptive events of historical proportions in terms of Sun-to-Earth transit time and heliospheric impact. The November 2004 events were marked by very fast CMEs and super storms in Earth's magnetosphere. The January 20, 2005 event was distinguished by the largest ground level enhancement (GLE) of solar cycle 23 (Gopalswamy et al., 2005b). Finally, the September 2005 period was marked by a very high rate of flare production in a two-week period. These events overlapped with the recent campaign of the Climate and Weather of the Sun Earth System (CAWSES) program. In the following section, we shall describe the geoeffectiveness and SEPeffectiveness of the CMEs, and the flare productivity of the underlying active regions.

2.1 October-November 2003 events

Key aspects of solar eruptions and space weather effects (including active region size and potential energy, flare occurrence rate and peak intensity, CME speed and energy, shock occurrence rate, SEP occurrence rate and peak intensity, geomagnetic storm intensity) for the episode of intense solar activity in late October - early November 2003 have already been reported (Gopalswamy et al., 2005c). Shock transit times for the Oct-Nov 2003 events and documented historical cases are used to infer a minimum CME Sun-Earth transit time and it is argued that this minimum transit time (maximum CME speed) is consistent with the free energy available from active regions.

The October – November 2003 activity was contributed by three active regions, AR 484, 486, and 488, of which AR 486 was the most intense. Most of the SEPeffective and geoeffective events were produced by this region. An unusually large fraction of fast and wide CMEs and halo CMEs occurred during this period. Sixteen shocks were identified near the Sun using radio data, while eight of them were intercepted by spacecraft along the Sun-Earth line. Two of these shocks arrived at Earth in < 20 h, making them part of a set of only 13 other fast-transit events reported since 1859 (the Carrington event). CMEs occurring near the disk center resulted in intense geomagnetic storms; some of them among the largest ones of solar cycle 23 (Gopalswamy et al., 2005d).

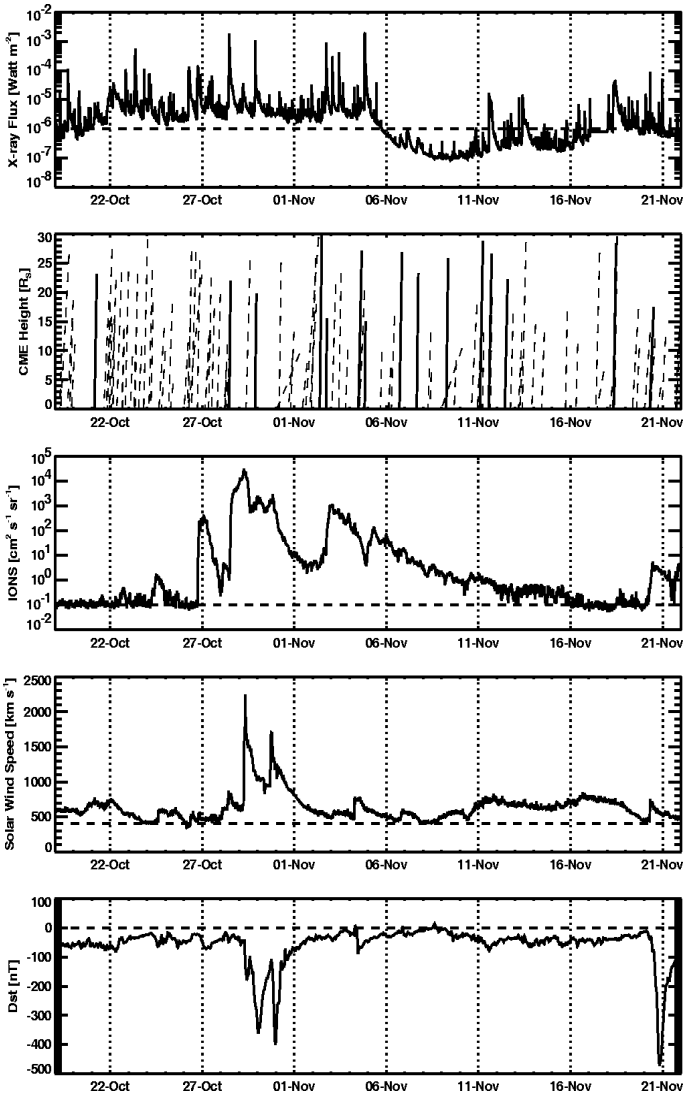

Fig. 2. GOES X-ray light curve, CME height-time plots, SEP flux (of > 10 MeV protons), 1-AU solar wind speed from ACE, and the Dst index for the Oct-Nov 2003 interval. GOES C-class flares and the nominal quiet conditions in other measurements are marked by the horizontal dashed lines. Solid lines in the height-time plots represent halo CMEs.

Very intense SEP events, including three ground level enhancements (GLEs) occurred in association with the CMEs. The extreme CME kinetic energy is consistent with the largest energy extractable from the huge active regions. One of the CMEs from AR 486 on 2003 October 28 had a kinetic energy of $1.2x10^{33}$ erg. The energy in the SEPs in each of the major events ranged from ~125% of the CME kinetic energy (Mewaldt et al., 2005). The highly energetic protons associated with the SEP events penetrated into the mesosphere and stratosphere where they produced strong depletion of Ozone by 50-70% (Jackman et al., 2005). The Ozone depletion was attributed to the enhanced production of HOx (H, OH, HO2) and NOx (NO and NO2) by energetic solar protons.

The majority of the reporting spacecraft and about 18% of the onboard instrument groups were affected by the Oct-Nov 2003 events one way or the other (Barbieri et al., 2004). Electronic upsets, housekeeping and science noise, proton degradation to solar arrays, changes to orbit dynamics, high levels of accumulated radiation, and proton heating were observed. Space weather awareness prompted putting most Earth-orbiting spacecraft into safe mode to protect from the particle radiation. The direct impact on the society was felt in southern Sweden (Malmoe) where about 50,000 people experienced a blackout. This was attributed to heating up the transformer oil by 10 degrees. The October-November 2003 events had significant impact on other parts of the heliosphere also: the MARIE instrument on board the Mars Odyssey succumbed to the SEPs. The interplanetary disturbances continued to the orbits of Jupiter and Saturn as detected by Ulysses and Cassini, respectively. Finally, the disturbances reached Voyager 2 after about 180 days, piled up together as a single merged interaction region (MIR), which led to a large depression in cosmic ray intensity, lasting more than 70 days (Richardson et al., 2005).

2.2 November 2004 events

The November 2004 activity originated in AR 0696 with two spurts: the first one was weak with a few halo CMEs and low level SEP flux. The main activity started when the region was at N09W17 on November 7th with an X2 flare, and a 1759 km/s CME. There were several halo CMEs on 2004 November 6, 7, 9, and 10 and each one of them was associated with a particle event (see Fig. 3). The halos were very fast, with speeds of 818 km/s (Nov. 6), 1759 km/s (Nov. 7), 2000 km/s (Nov. 9) and 3387 km/s (Nov. 10). Two other slower halos must have added to the complexity of the IP disturbances of this interval. The last CME had the highest average sky-plane speed in cycle 23. The SEP intensity remained above 10 pfu level for about a week and the highest intensity (495 pfu) occurred following the Nov 7 halo at 17:06 UT. The solar wind speed also remained elevated for several days in association with four shocks and three magnetic clouds. The magnetic clouds resulted in two super-intense storms (373 nT and 289 nT). The first storm is clearly associated with the Nov. 6 halo. This halo was also preceded by another halo of moderate speed (818 km/s) from the same region. The magnetic storm must have been produced by the merged structure of the two CMEs. Fig. 4 shows a LASCO image showing the complex structure consisting of the two CMEs and the GOES plot showing multiple eruptions. There was a single shock associated with the two CMEs, but the ICME was quite extended. The second storm on Nov. 10 is most likely due to the halo on Nov. 07 at 16:54 UT. There were two shocks preceding the storm-causing magnetic cloud. Further investigation is needed to identify the sources of the two shocks.

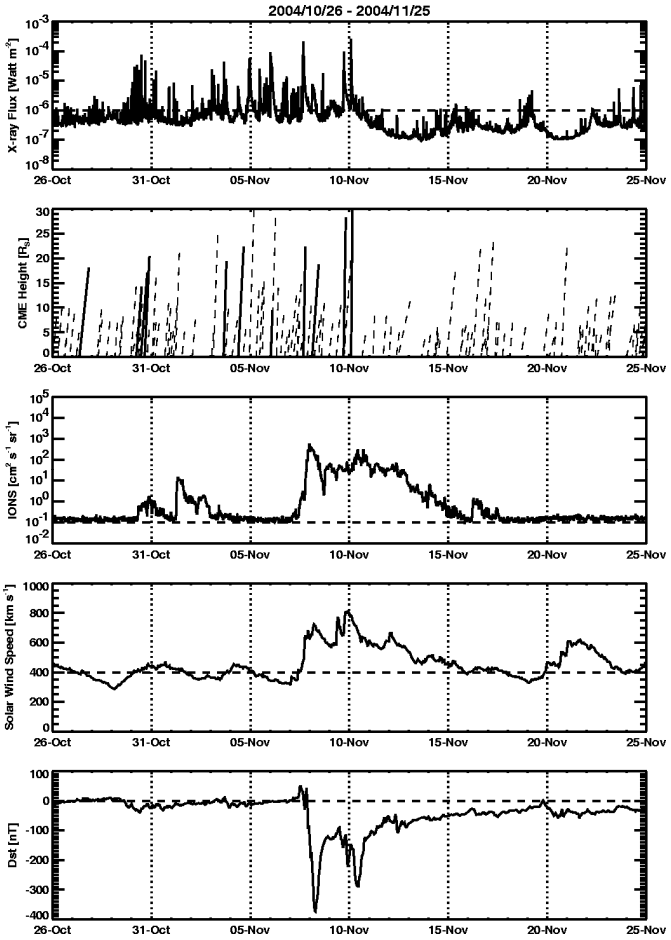

Fig. 3 Summary plot as in Fig. 2, for the 2004 Nov. interval.

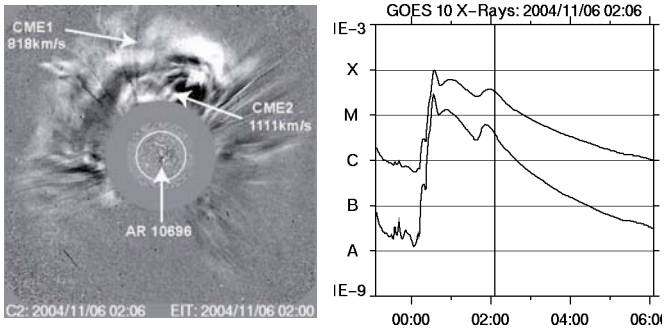

Fig. 4. (left) SOHO/LASCO image showing two CMEs. (right) GOES X-ray light curve indicating multiple eruptions. The time of the LASCO image is marked by the vertical line.

2.3 January 2005 events

The January 2005 events originated from AR 0720. The region developed in the northwest quadrant of the Sun and produced the first flare on Jan. 11. Initially, the flares were weak (GOES B and C class) and then started producing larger flares when the AR grew in size (see Fig. 5). The first X-flare occurred on Jan. 15 and the last one was on Jan. 20. There were seven full halos, each one associated with an SEP event. The SEP intensity remained above 10 pfu for seven days. The largest SEP event had an intensity of 5070 pfu associated with the Jan. 17 CME. This was an ultrafast (speed 2547 km/s) halo CME interacting with another ultrafast (2094 km/s) CME event. The onsets differed by only 37 min. The first CME was followed by just a brief SEP event. The solar wind

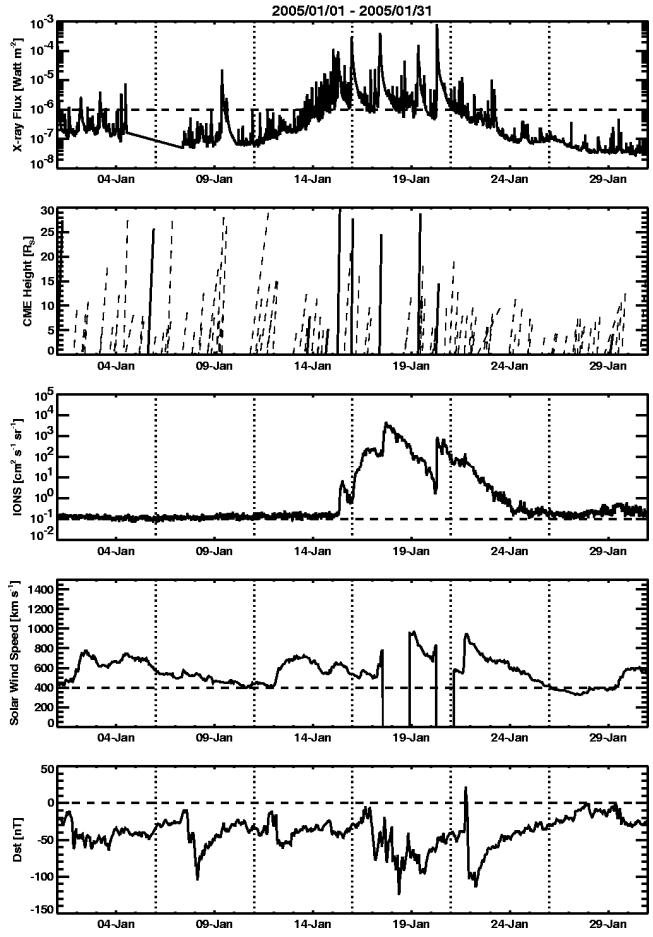

Fig. 5. Summary plot as in Fig. 2, for the 2005 Jan interval.

measurements had several data gaps, but the speed was relatively high. The geomagnetic storms were of only moderate intensity. Although the Dst index showed weak activity for several days starting from Jan 17, the index dipped to -100 nT only briefly on two occasions. The second storm was associated with the Jan 20 CME, which was also associated with a large SEP event that had ground level enhancement (GLE). The GLE event also happened to be the largest of solar cycle 23 (Gopalswamy et al., 2005b). The CME was clearly seen only in one frame. Combining with the SOHO/EIT image, it was possible to estimate the sky-plane speed as 3242 km/s, very close to the November 10 event.

2.4 September 2005 events

Active region 808 was already active in producing frequent flares as it rotated on to the disk on Sep. 5. During the disk passage, it produced 10 X flares, 24 M flares, and a large number of smaller flares. When the region arrived at the disk center, the activity weakened. The first large flare was an X17 flare when the region was at the east limb (S03E89) on Sep 7.

Unfortunately, there was a LASCO data gap from 10:42 UT on Sep. 7 through 12:21 UT on Sep. 9. Therefore, any CME associated with this huge flare must have been missed. However, there was an intense type II burst in the corona and IP medium as well as a shock at 1 AU observed on Sep. 9 at 13:10 UT. All these indicate that a very energetic CME must

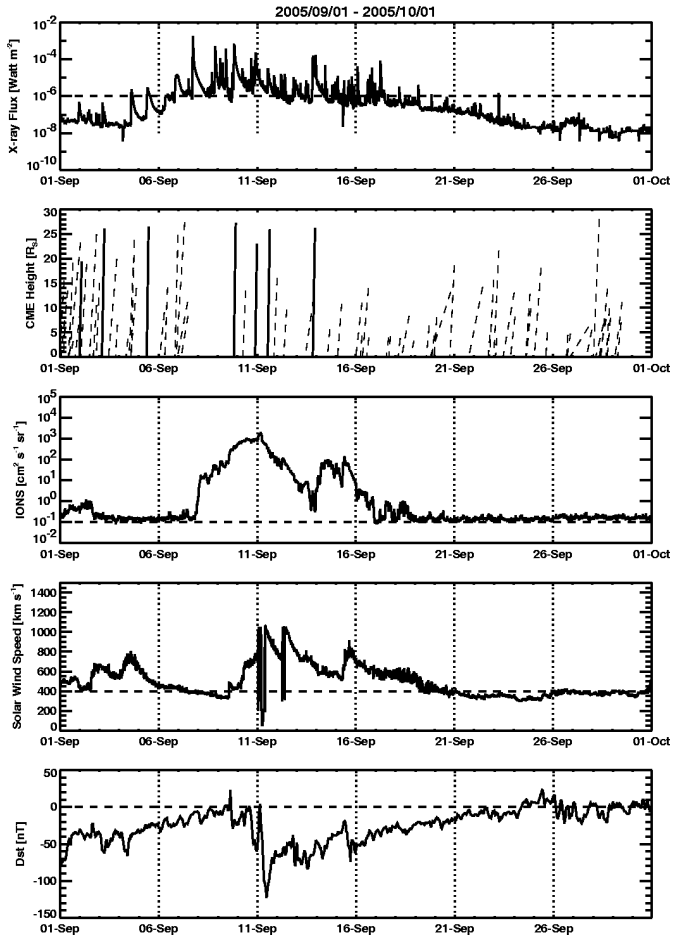

Fig. 6. Summary plot as in Fig. 2, for the 2005 Sep interval.

have been present, but missed due to the data gap. There were 7 other halo CMEs. The four halos after the X17 flare (Sep 7) were all associated with SEP events. The SEP intensity remained above 10 pfu level for about 8 days. The last X-class flare on Sep. 15 at 8:30 UT was not associated with a CME. The interval had 9 CMEs with speed exceeding

1000 km/s (two had speed > 2000 km/s). The geoeffectiveness of these events were rather poor, probably because most of the CMEs originated from the eastern hemisphere.

3. Intercomparison of the four intervals

Table 1 summarizes the activities from the four ARs. All the regions are geoeffective and SEPeffective, but to different degrees. These two space weather consequences have different requirements for CMEs (Gopalswamy et al., 2006; Gopalswamy, 2006). For geoeffectiveness, the CME plasma has to reach Earth's magnetic field with a southward magnetic field component. For producing SEPs, the CMEs have to drive shocks and the shock-accelerated particles have to be magnetically connected to the detecting spacecraft. The SEP-producing CMEs are generally much faster than the geoeffective CMEs (Gopalswamy et al., 2004) although both have above average speeds. The geoeffective CMEs are generally located close to the disk center, whereas the SEPeffective CMEs originate more on the western hemisphere. For SEP production, CMEs have to drive strong shocks irrespective of the internal magnetic structure.

The AR area (expressed millionths of solar hemisphere, or msh) is the largest for AR 486 and the smallest for AR 696. The areas are well above the median value (800 msh) of the area distribution for SEP-producing regions of cycle 23 (Gopalswamy et al., 2005c). The flare productivity is also the smallest for AR 696 and highest for AR 486. All the regions produced roughly the same number of full halo CMEs. At least two CMEs from each AR had speeds > 2000 km/s. The Dst index of the storms from ARs 486 and 696 were at the superintense level, whereas ARs 720 and 808 had only modest storms. The SEP intensity remained at a hazardous level for 6-13 days. However, the peak intensity of > 10 MeV protons varied over two orders of magnitude. The number of IP shocks is also the largest for AR 486. The area of AR 696 was about one third of that of AR 486, yet the Dst index due to CMEs from the two regions were comparable. The reason for the different geoeffectiveness can be traced to the location of the eruption regions at the time of the concerned CMEs. AR 696 was closest to the disk center when the storm-causing CMEs erupted. The latitude was ~ N09. AR 720 was slightly at higher latitudes and more westerly (W58) when the CME erupted. AR 808 had latitudes similar to those of AR 696 but the CMEs occurred when the AR was close to the east limb. AR 486 was very close to the disk center (S20E02 and S19W09 on Oct 28 and 29, respectively) even though the latitude was slightly high. However, AR 486 had a trans-equatorial connection to AR 488 in the north, so the CMEs were effectively heading towards Earth (see Gopalswamy et al., 2005c for details). The effect of the distance of the active region from the Sun center also reflected in the appearance of the halos as symmetric or asymmetric. The Jan and Sep 2005 halos were more asymmetric compared to the other two. While the location of the eruption on the Sun is very important, one has to consider propagation effects such as interaction with the solar wind and other CMEs (Manoharan et al., 2004; Schwenn et al., 2005).

Table 1. Comparison of Eruptions from the Four Regions

AR #	486	696	720	808
Interval	10/18-11/7 03	11/2 – 11/13 04	01/11 - 01/23 05	09/05-09/19 05
Area (msh)	2610	910	1630	1430
X/M flare	7/23	2/13	5/19	11/20
Full Halos	7	7	8	7
Fast CMEs	14 (5)	6(2)	7 (6)	8 (2)
< -100 nT	3 events	2 events	2 events	1 event
Dst (-nT)	363, 401	373, 289	121, 105	123
>10 pfu	13 days	6 days	7 days	8 days
SEP pfu	33,600	495	5040	1880
IP Shock	7	5	1	3

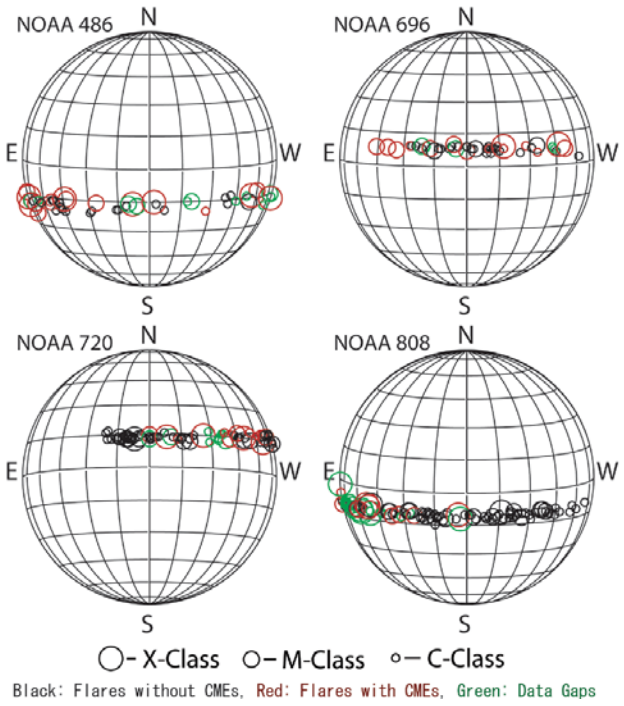

Fig. 7. Heliographic locations of flares from the four active regions: 486, 696, 720 and 808.

4. Summary and conclusions

We have presented a preliminary analysis of 4 active regions that were geoeffective and SEP effective during the declining phase of solar cycle 23. The solar origin and geospace consequences of the four sets of events were well observed,

so we have an extremely rich data set, which has the potential of yielding a lot of information for space weather applications. CMEs from all regions were SEPeffective, however, only two of them were very geoeffective. This demonstrates the different requirements for SEPeffectiveness and geoeffectiveness. Understanding the behavior of such super active regions is very important for prediction purposes.

Acknowledgments. We thank S. Petty for checking the manuscript. This research was supported by NASA's SR&T and LWS TR&T programs.

References

L. P. Barbieri and R. E. Mahmot, *Space Weather*, vol. 2, S09002, 2004.

C. M. S. Cohen, in *Solar Eruptions and Energetic Particles*, N. Gopalswamy R. Mewaldt and J. Torsti, Eds. AGU GM, Washington, DC, in press.

N. Gopalswamy, in *The Sun and the Heliosphere as an Integrated System*, ASSL, G. Poletto and S. Suess, Eds. Kluwer, Boston, 2004, pp. 201-252.

N. Gopalswamy, J. *Astrophys Astron.*, in press, 2006.

N. Gopalswamy, L. Barbieri, E. W. Cliver, G. Lu, S. P. Plunkett and R. M. Skoug, *J. Geophys. Res.*, vol. 110, A09S00, 2005a.

N. Gopalswamy, B. Fleck and J. B. Gurman, in *Proc. of Asia Pacific Regional Conf. of IAA "Bringing Space Benefits to the Asia Region"*, R. Mukund and R. Murthy, Eds. in press, 2006.

N. Gopalswamy, H. Xie, S. Yashiro and I. Usoskin, in *Proceeding of 29th International Cosmic Ray Conference*, Pune, 2005b.

N. Gopalswamy, S. Yashiro, S. Krucker, G. Stenborg and R. A. Howard, *J. Geophys. Res.*, vol. 109, p. 12105, 2004.

N. Gopalswamy et al., *J. Geophys. Res.*, vol. 110, A09S15, 2005c.

N. Gopalswamy, S. Yashiro, G. Michalek, H. Xie, R. P. Lepping and R. A. Howard, *Geophys. Res. Lett.*, vol. 32, p. 12, 2005d.

J. T. Gosling, *J. Geophys. Res.*, vol. 98, pp. 18937-18949, 1993.

R. A. Howard, D. J. Michels, N. R. Sheeley Jr. and M. J. Koomen, *Astrophys. J.*, vol. 263, pp. L101-L104, 1982.

C. H. Jackman, et al., *J. Geophys. Res.*, vol. 110, A09S27, 2005.

P. K. Manoharan, N. Gopalswamy, S. Yashiro, A. Lara, G. Michalek and R. A. Howard, *J. Geophys. Res.*, vol. 109, A06109, 2004.

R. Mewaldt, et al., *J. Geophys. Res.*, vol. 110, A09S18, 2005.

D. V. Reames, *Space Sci. Rev.*, vol. 90, p. 413, 1999.

J. D. Richardson, C. Wang, J. C. Kasper and Y. Liu, *Geophys. Res. Lett.*, vol. 32, L03S03, 2005.

R. Schwenn, A. Dal Lago, E. Huttunen and W.D. Gonzalez, *Ann. Geophys.*, vol. 23, p. 1033, 2005.

B. T. Tsurutani, W. D. Gonzalez, F. Tang, S. I. Akasofu and E. J. Smith, *J. Geophys. Res.*, vol. 93, pp. 8519-8531, 1988.

D. F. Webb, E. W. Cliver, N. U. Crooker, O. C. St. Cyr and B. J. Thompson, *J. Geophys. Res.*, vol. 105, pp. 7491-7508, 2000.